Available online at www.sciencedirect.com
SCIENCE DIRECT®
Computer Physics Communications 164 (2004) 377–382
Computer Physics Communications
www.elsevier.com/locate/cpc

Modeling plasma-wall interactions in First Wall-Limiter geometry

F. Subba [*,1], R. Zanino

Dipartimento di Energetica, Politecnico, I-10129 Torino, Italy

Available online 21 July 2004

Abstract

We test the standard edge plasma code B2-solps5.0 on a model First-Wall Limiter (FWL) geometry. The presence of a tangency point between the solid wall and the magnetic separatrix introduces a singular point in the geometry. A quadrilateral computational mesh can fit the given configuration only if it is highly distorted, constituting a severe test for any numerical scheme. The original 5-point molecule adopted by B2-solps5.0 fails to solve the plasma transport equations near the singular point. A correction scheme is proposed, which is equivalent to adopting a 9-point stencil.

Keywords: Numerical methods; Edge modeling; Tokamak

1. Introduction

First-Wall Limiters (FWL) have been proposed to handle the power loads on the Plasma Facing Components (PFC) of fusion devices, e.g., in the IGNITOR design [1]. Although the concept is not new [2], most present Tokamaks are diverted [3], so that comparatively little experience exists on the advanced modeling of limited plasmas [4,5]. A FWL presents severe modeling problems, due to the presence of a tangency point between the magnetic separatrix and the physical wall. The most advanced edge simulation codes employ quadrilateral grids, and the strong plasma anisotropy demands to align the grid cells with the magnetic surfaces. Under these conditions, the construction of a suitable mesh becomes a major challenge.

We test a popular edge plasma code, B2-solps5.0 [6], on a model problem in FWL geometry. The code adopts a 5-point computational stencil, which may cause problems for a very distorted grid, as is needed to fit the FWL configuration. Then, we discuss a simple method to effectively switch to a 9-point scheme without changing dramatically the structure of the linear solver implemented. The main idea of the procedure goes back to the seventies [7] but, to the best of our knowledge, it was never applied to edge Tokamak modeling. It can provide an efficient way to improve the commonly adopted schemes. In Section 2 we illustrate our model geometry and discuss a method to fit a quadrilateral mesh. In Section 3 we analyze the 5-point stencil of B2-solps5.0, and determine its properties on distorted grids. In Section 4 we illustrate some curvilinear test cases, outlining issues resulting from numerical experiments. In Section 5 we propose a cor-

* Corresponding author.
E-mail address: fabio.subba@polito.it (F. Subba).
[1] Supported by the Associazione per lo Sviluppo Scientifico e Tecnologico del Piemonte, Torino, Italy.

0010-4655/$ – see front matter
doi:10.1016/j.cpc.2004.06.050

rection to the computational molecule, including the grid skewness, and discuss some examples. Finally, in Section 6 we summarize our results and draw our conclusions.

2. Geometry and mesh

B2-solps5.0 is a 2D multi-fluid code based on the Braginskii model [8]. Its 5-point stencil is optimized if the following hypothesis are satisfied: (i) the domain is parameterized with 2 curvilinear orthogonal coordinates, one of which (poloidal) lies on the magnetic surfaces and the other, (radial) labels the surfaces themselves, and (ii) the domain boundaries are coordinate lines. Then the domain can be mapped onto a rectangle, whose sides correspond to the poloidal (x) and radial (y) coordinates.

5-point stencils are attractive in many respects [9], but may be inaccurate if (i) or (ii) are violated. In the applications, it is often difficult to meet both (i) and (ii). In diverted machines, target plates are tilted with respect to the magnetic field, to reduce the heat load, and the mesh must be deformed to fit the actual PFC shape. For a FWL, the same problem appears at the tangency point, but is much more severe because the transformation to a co-ordinate system aligned with the magnetic field and following the wall is singular. As an example, in Fig. 1 we illustrate the logical mapping of an edge plasma onto a rectangle in the standard divertor case (left) and in our model FWL geometry (right), where up–down symmetry was assumed. For the latter case, the magnetic surfaces are circles concentric with arcs AD and FE. A similar, somewhat simpler, case was studied in [10].

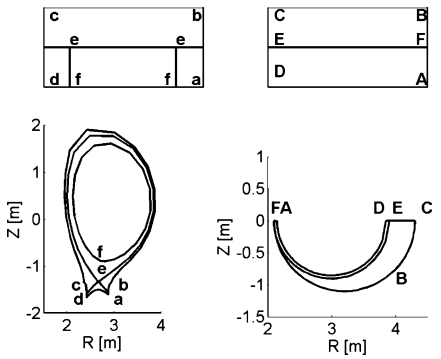

Fig. 1. Logical mapping of a physical domain onto a rectangle. Left: a standard divertor case. Right: an FWL geometry.

To generate a quadrilateral grid in the SOL region (FBCEF) is possible, but it is intuitively clear the cells must be extremely distorted near the tangency point B. Leaving apart the technical details of the grid generation algorithm, we show in Fig. 2 the mesh structure near the tangency point. We measure the grid distortion with the skewness SK, which we define for cell (i, j) as:

$$SK_{i,j} = 1 - \left(\sum \sin(\alpha_m)\right)/4. \tag{1}$$

3. Influence of the 5-points stencil

As discussed in Section 1, B2-solps5.0 adopts a 5-point stencil. The performances of such a scheme degrade for extremely distorted grids such as that shown in Fig. 2. Here we analyze the scheme used, aiming at assessing how it interacts with the grid distortion.

We consider, for the sake of simplicity, a region of space with a uniform magnetic field aligned to the x-direction, and neglect any curvilinear effects. With this setup, the magnetic field defines the direction of strong transport, but does not appear explicitly in the equations.

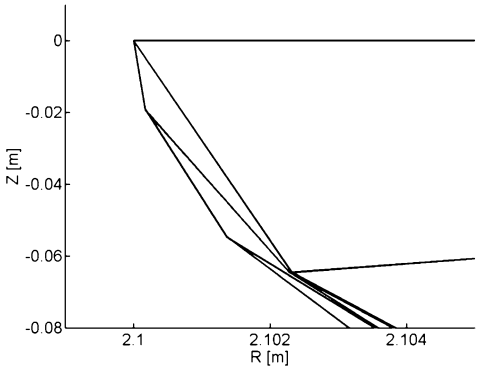

Fig. 2. Structure of a mesh near the tangency point. Note the all the elements are quadrilateral, even if some of them look triangular on the scale of the picture.

B2-solps5.0 solves a set of coupled fluid equations, each of which can be written in the general form:

$$\frac{\partial \phi}{\partial t} + \frac{\partial}{\partial x}\left(\phi \alpha_x v_x - D_x \frac{\partial \phi}{\partial x}\right) + \frac{\partial}{\partial y}\left(\phi \alpha_y v_y - D_y \frac{\partial \phi}{\partial y}\right) = \frac{\partial \phi}{\partial t} + L(\phi) = S(\phi), \quad (2)$$

where the symbol ϕ stands for the charged species density, velocity, temperature or plasma potential. In the homogeneous stationary case, Eq. (2) reduces to $L(\phi) = 0$. At each node (i, j) the previous equation is substituted with the discrete approximation:

$$\widehat{L}_{i,j}(\widehat{\phi}) = \sum_{p=-1,k=-1}^{p=1,k=1} a_{p,k}^{i,j} \widehat{\phi}_{i+p,j+k} = 0, \quad (3)$$

where $\widehat{L}_{i,j}$ and $\widehat{\phi}$ are the discrete representations of L and ϕ, respectively.

We take as an example now the electron energy equation, and make the additional simplification of constant coefficients. Although this is a major departure from the properties of real plasmas, the qualitative conclusions that will follow are independent from the variation of the electron heat conductivity χ with the plasma conditions. Having said this, we identify ϕ with the electron temperature T, D with χ, and write $\alpha_{(x,y)} = 1.5n$, n being the electron density. The coefficients $a_{p,k}^{i,j}$ are collected in Table 1, where we set $G_{x(y)} = 1.5 n v_{x(y)}/h_{x(y)}$ and $H_{x(y)} = \sqrt{(G_{x(y)}/2)^2 + (\chi_{x(y)}/(h_{x(y)})^2)^2}$. The geometrical factors $h_{x(y)}$ are the grid spacing along the co-ordinate x- and y-directions.

Developing the temperature $T_{i+p,j+k}$ using Taylor's formula, and taking into account the grid distortion, we obtain that the numerical scheme implemented is actually consistent with:

$$L(T) = \frac{\partial}{\partial x}\left(\left(1.5 n v_x + 1.5 n v_y \tan(\theta)\right)T - \left(\chi_x + \chi_y \tan^2(\theta)\right)\frac{\partial T}{\partial x}\right) + \frac{\partial}{\partial y}\left(1.5 n v_y T - \chi_y \frac{\partial T}{\partial y}\right) - 2\tan(\theta)\chi_y \frac{\partial^2 T}{\partial x \partial y} \quad (4)$$

which shows clearly the effect of the grid distortion, amounting to the artificial introduction of terms proportional to $\tan(\theta)$ and $\tan^2(\theta)$. Under typical edge plasma transport conditions we have $n v_y \ll n v_x$ and $\chi_y \ll \chi_x$ [11], which evidently lessens the problem of the additional spurious terms until θ does not become too large. For the test case shown in the previous section we pushed the distortion up to values $\tan(\theta) \leqslant 10^3$, in order to fit the tangency point. In order to assess more quantitatively the relevance of the spurious terms, we concentrate on the one growing fastest in Eq. (4), $\propto \chi_y \tan^2(\theta)$. It is natural to evaluate its importance using the dimensionless parameter $\sigma = \chi_y \tan(\theta)^2/\chi_x$. In evaluating what σ can be for a real modeling case, we should identify χ_x with the poloidal conductivity, and χ_y with the radial one. In Fig. 3 we show the variation of σ as the grid distortion increases towards extreme values. Two lines are reported. The lower one assumes a value of χ_x similar to the poloidal conductivity of a plasma at $T \approx 10$ eV and a ratio $B_p/B \approx 0.1$ for the poloidal to total magnetic field, while the upper one considers the case $T \approx 1$ eV [11]. As expected from the previous analysis, we can see that the lower temperature case is more sensitive to the grid distortion. The spurious terms in

Table 1
Structure of the 5-point stencil employed by B2-solps5.0

	$i=-1$	$i=0$	$i=1$
$j=-1$	0	$-0.5G_y - H_y$	0
$j=0$	$-0.5G_x - H_x$	$2(H_x + H_y)$	$0.5G_x - H_x$
$j=1$	0	$0.5G_y - H_y$	0

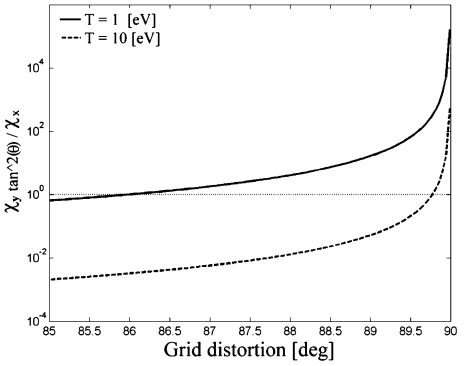

Fig. 3. Relative importance of the largest spurious terms introduced by the grid distortion, measured by the parameter $\sigma = \chi_y \tan^2(\theta)/\chi_x$ for two values of the parallel conductivity, assuming $T_e = 1$ eV (solid line) and $T_e = 10$ eV (dashed line). The horizontal lines marks the level where the unphysical terms introduced by the mesh distortion becomes dominant.

the transport equation start being comparable with the physical ones for a distortion of about 86°, and later on become quickly dominant. At the higher temperature, the scheme can tolerate a much larger distortion without severe effects.

In the general case of edge Tokamak plasma modeling, the extreme conditions required to seriously deteriorate the scheme properties may be sometimes marginally found. In diverted Tokamaks it is common to build the divertor targets nearly parallel to the magnetic field, in order to reduce the peak power load on the solid components. It could then be possible that some not negligible effect appeared near the plates, especially when modeling very low temperature (detached) plasmas; this is probably an issue to be considered on a case-by-case basis. As far as the FWL geometry is concerned, the problem is much more dramatic. We already mentioned that in order to fit the tangency point we pushed the grid distortion up to $\tan(\theta) \leqslant 10^3$. Under such conditions we expect that our simulations should definitely show some distortion effects. In the next section we will describe the results of a few numerical experiments performed in the full curvilinear FWL geometry.

4. B2 test on FWL geometry

We describe the results of numerical experiments on an FWL geometry. As a reference case, we studied a pure D plasma in a domain with minor radius $a = 0.9$ m, and extending in the inner plasma for 1.5 cm. The magnetic field poloidal and toroidal components are $B_T = 13$ T and $B_p = 2.5$ T, respectively. We set at the inner plasma boundary (tract AD of Fig. 1) $n = 10^{20}$ m^{-3}, and $T_e = T_i = 50$ eV. In order to impose the boundary conditions to the FWL (tract FB in Fig. 1), we treat it as a standard target, and apply the sheath theory, ignoring the singularity of the tangency point for the sake of simplicity (the difficult and possibly open issue of an adequate boundary condition for the transition region between finite angle of incidence and tangency point is beyond the scope of the present paper, see [13] for a treatment of the sheath problem in the degenerate case of field parallel to the wall). Far from the tangency point, along tract BC, we set zero radial particle flux and temperature decay length (1 m). Along tracts FA and DC we impose symmetry conditions. Both the heat and particle radial diffusivities, are 1 m^2 s^{-1}, the parallel transport is classical [8].

Fig. 4 shows the effect of a poloidal grid refinement on the computed heat flux along the FWL. The solution converges towards a mesh-independent profile, except in a narrow region (≈ 5 cm), near the tangency point at zero abscissa. The inset is a zoom on the critical tangency region, to better appreciate the differences. For a completely converged solution we should expect the heat flux to vanish at the tangency point, because the sheath condition imposes $\vec{q} \cdot \vec{n} \propto c_s T \cos(\beta)$ where β is the angle between the magnetic field and the normal to the wall. The convergence study should be completed by refining the mesh also radially. However, from the previous section we see that this very process would be ambiguous. An excessive grid refinement near the tangency point would increase the grid distortion (the quadrilateral cells would tend to degenerate). From Eq. (4), after a threshold, the terms depending on $\tan(\theta)$ becomes dominant, leading to the solution of *different* equations on different grids. By numerical experiment, it was found that attempting further radial refinements drives the code unstable. The heat flux profile further on along the limiter is much more regular and grid-independent. This is a strong suggestion, even if not a proof, that the perturbation near the tangency point does not propagate to pollute the solution globally. The approximate for-

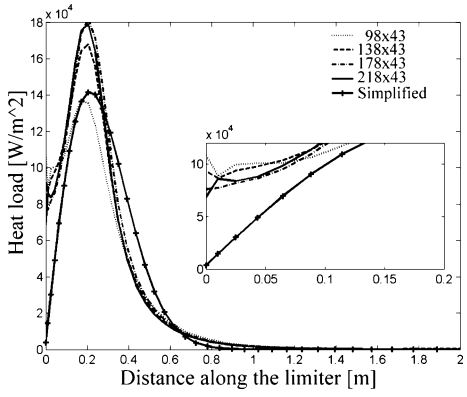

Fig. 4. Heat flux profiles along the FWL from a series of grids with increasing poloidal refinement. The results of a semi-analytic simplified model is also reported for comparison. (Inset: zoom of the different profiles near the tangency point.)

mula [12]

$$q(s) = q_0 e^{(-l/\lambda_E)} \cos(\beta) \tag{5}$$

is commonly adopted to estimate the heat load on the Plasma-Facing Components in FWL geometry for engineering purposes. In Eq. (5) q_0 is a normalization factor, l is the distance between the separatrix and the wall, λ_E is the radial energy decay length. The heat flux profile obtained with Eq. (5) is also shown in Fig. 4 for a qualitative comparison.

5. Scheme correction

We discuss a possible modification to the B2-solps5.0 scheme, to correct for the grid distortion. In order to simplify the analysis, we make the further assumption of zero plasma velocity and concentrate on the diffusive terms. The most natural way to correct Eq. (4) would be to implement a 9-point computational molecule. For example, it can be shown that the scheme becomes consistent if to the discrete operator $\widehat{L}$ defined in Section 3 we add $\widehat{K} = \chi_y(\tan(\theta)\widehat{K_1}/2h_x h_y + \tan(\theta)^2\widehat{K_2}/h_x^2)$ where the two additional computational molecules are:

$$\widehat{K_1} = \begin{pmatrix} -(1+2r) & 4r & (1-2r) \\ 1 & 0 & -1 \\ 0 & 0 & 0 \end{pmatrix},$$

$$\widehat{K_2} = \begin{pmatrix} 0 & 0 & 0 \\ 1 & -2 & 1 \\ 0 & 0 & 0 \end{pmatrix}. \tag{6}$$

It is not necessarily desirable to move to a 9-point stencil, because of the significant programming effort required. In order to avoid solving a larger system of algebraic equations, we can think of treating explicitly the additional operator $\widehat{K}$. To show the effect our procedure, we solved the test equation on a skewed domain, shown in Fig. 5. It represents schematically a single flux tube ending to a solid surface along the boundary AD. Along BC we fixed the temperature, while at the opposite extreme, AD, we set $k_x \partial T/\partial x \propto T^{1.5}$. Along AB and CD we set the simplest possible conditions: $\partial T/\partial \xi = 0$, where ξ is the skewed direction. For an orthogonal grid, this corresponds to zero perpendicular flux. For a skewed grid we kept it because of its simplicity. Fig. 6 shows correction for a distortion of 89° for two different maximum temperatures: $T_{\max} = 10$ eV and $T_{\max} = 15$ eV. The difference between the corrected and not corrected case is clear at the lower temperature, but if we increase $T_{\max}$, the two solutions becomes indistinguishable. However, pushing the grid distortion up to 89.5°, the correction effect

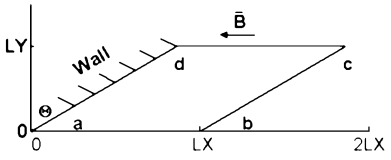

Fig. 5. Schematic representation of the domain used to test the correction for the grid distribution.

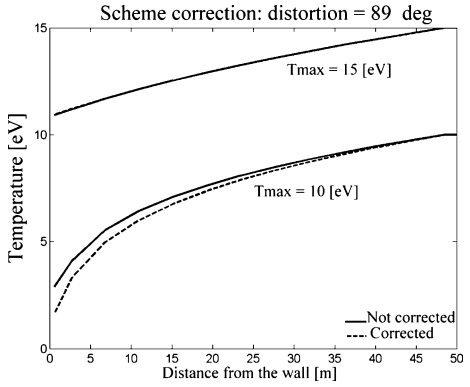

Fig. 6. Effect of the correction for a grid distortion of 89°. For a low temperature case, $T_{\max} = 10$ eV, the temperature profiles is sensitively different depending on having corrected the scheme for the grid distortion or not. For a higher temperature case, $T_{\max} = 15$ eV, the correction becomes influent.

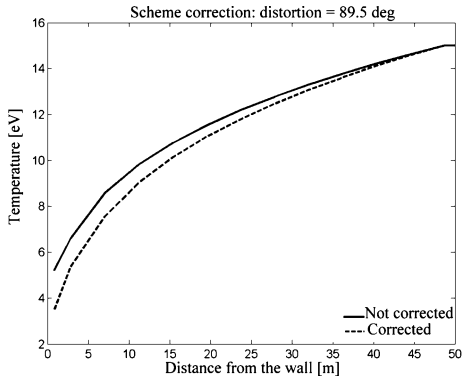

Fig. 7. Effect of the correction for a high grid distortion 89.5°. The correction effect is noticeable also for a large temperature case.

becomes noticeable for T_{max} as high as $T_{max} = 15$ eV, Fig. 7.

6. Conclusions

We analyzed the potentialities of the B2-solps5.0 code for studying the Scrape-off Layer in FWL configuration, as is planned, e.g., for IGNITOR. We showed that a quadrilateral mesh fitting the magnetic geometry grid can be built in the neighborhood of the tangency point, provided we tolerate substantial grid distortions. The 5-point scheme adopted by B2-solps5.0 is not designed to operate on distorted grids. However, if one line co-ordinate is aligned with the dominant transport direction and the transport itself is sufficiently anisotropic, the inaccuracy of the scheme is small except near the tangency point. A relation has been derived quantitatively analyzing the importance of the distortion, and finding the marginal condition for which it becomes relevant. For standard edge Tokamak modeling, the above requirements may be sometimes met in case of extremely tilted target plates and very low temperature plasma (detached). For a FWL configuration, the distortion effect becomes dominant near the tangency point, and contributes to severely deteriorate the quality of the solution there. We proposed a method to correct for the grid distortion without resorting to a 9-point algebraic solver. Numerical experiments showed the effect of the correction in simple test cases. This is encouraging in view of coupling our algorithm with the full system of equations solved by B2-solps5.0.

References

[1] B. Coppi, et al., Critical physics issues for ignition experiments, MIT RLE Report, PTP 99/06, 1999.
[2] C. Ferro, et al., Limiter and X-point configurations in ignition experiments, in: Proceedings of the 28th EPS Conference on Controlled Fusion and Plasma Physics, Funchal, PO, 2001.
[3] C.S. Pitcher, P.C. Stangeby, Plasma Phys. and Contr. Fusion 39 (1997) 779.
[4] M. Baelmans, et al., J. Nucl. Mater. 290–293 (2001) 537.
[5] D.S. Gray, et al., Phys. of Plasmas 6 (1999) 2816.
[6] R. Schneider, et al., Contrib. Plasma Phys. 40 (2000) 423.
[7] P.K. Khosla, S.G. Rubin, Contrib. Comput. Fluids 2 (1974) 207.
[8] S.I. Braginskii, Transport processes in a plasma, in: Reviews of Plasma Physics, vol. 1, Consultants Bureau, New York, 1965.
[9] J. Ferziger, M. Peric, Computational Methods for Fluid Dynamics, Springer, 2002.
[10] B. Braams, Numerical studies of the two-dimensional scrape-off layer, in: Proceedings of the 11th EPS Conference on Controlled Fusion and Plasma Physics, Aachen, GE, 1983.
[11] P.C. Stangeby, The Plasma Boundary of Magnetic Fusion Devices, Institute of Physics Publishing, 2002.
[12] C. Ferro, R. Zanino, ENEA Report RT/FUS/89/26.
[13] K. Theilhaber, C.K. Birdsall, Phys. Fluids B 1 (1989) 2260.